Processing and properties of boron carbide with hafnium Diboride addition

Sairam, K.; Sonber, J.K.; Murthy, T.S.R.C.H.; Paul, B.; Achiket, K.N.; Jothilakshmi, N.; Bedse, R.D.; Kain, V.

DOI:
10.13168/cs.2016.0049

Ceramics-Silikáty 60 (4), 330-337 (2016)
journal webpage: www.ceramics-silikaty.cz doi: 10.13168/cs.2016.0049

PROCESSING AND PROPERTIES OF BORON CARBIDE WITH HAFNIUM DIBORIDE ADDITION

#K. SAIRAM*, J. K. SONBER*, T. S. R. CH. MURTHY*, B. PAUL*, K. NACHIKET*, N. JOTHILAKSHMI**, R.D. BEDSE*, V. KAIN*

*Materials Group, Bhabha Atomic Research Centre, India
**Nuclear Fuels Group, Bhabha Atomic Research Centre, India

#E-mail: sairamk@barc.gov.in

Submitted June 22, 2016; accepted July 29, 2016

Keywords: Boron carbide; Hafnium diboride; Hot pressing; Mechanical properties; Electrical conductivity

This article presents the results of investigations on densification, mechanical and electrical properties of boron carbide (B_4C) with the addition of HfB_2. High dense B_4C-HfB_2 (2.5 - 30 wt .%) composites were prepared by hot pressing at a temperature of 2173 K with 40 MPa mechanical pressure. The B_4C-HfB_2 composite mixture exhibited a better sintering aptitude compared with monolithic B_4C. Hardness and elastic modulus of B_4C-HfB_2 composites were measured to be in the range 36 - 28 GPa and 465 - 525 GPa respectively. Indentation fracture toughness of B_4C increased with HfB_2 content and obtained a maximum of 7 MPa $m^{1/2}$ at 30 wt. % HfB_2, which is ~3 times higher than the monolithic B_4C. Crack deflection was identified to be the major toughening mechanism in the developed composite. B_4C – 10 wt. % HfB_2 composite exhibited a maximum electrical conductivity of 7144 Ω^{-1} m^{-1} which is 26 % higher than the conductivity of monolithic B_4C (5639 Ω^{-1} m^{-1}) at 1373 K.

INTRODUCTION

Boron carbide is a promising candidate for many high performance applications in nuclear and defence sectors because of its unique characteristics. A combination of low density (2.51 g·cm^{-3}), high elastic modulus (460 GPa) and high hardness (38 GPa) enables B_4C to find application in defence sector as an armour material. ^{10}B isotope of B_4C offers significant neutron absorption cross-section for both thermal and fast neutrons and thus plays a major role in nuclear industries as neutron detectors, control rods and shielding materials [1, 2].

Refractory nature of B_4C necessitates a high sintering temperature close to 2273 K which makes densification difficult and often deteriorates mechanical properties of the material due to the grain coarsening effects. Also, the extreme brittleness/poor fracture toughness of B_4C limits the wide spread application of the material [1, 3-6].

Different sintering methods that assists the densification of high temperature ceramics are the use of submicron particles, binder additions and adoption of advanced sintering process like spark plasma sintering (SPS) [1, 2, 7-18]. Most of the research work has been devoted towards binder based additions as it is reported to enhance both densification and mechanical properties of B_4C [7-17]. Sintering study by Skorokhod et al. has brought into focus the approach to explore different oxide based binder additions to lower the sintering temperatures and increasing the strength of B_4C [13]. It is reported that the chemical instability nature of B_4C with respect to oxide binders was favouring the formation of high dense B_4C-boride composite at comparatively lower sintering temperatures than that of monolithic B_4C [10, 19-22]. Till date, the ease of in-situ processing methodology overshadowed and limited the research on the densification of B_4C using pre-synthesized boride powders. In this study, hafnium diboride (HfB_2) is chosen as a ceramic binder, as it possesses attractive properties like high melting point, high hardness, high elastic modulus and neutron absorption cross-section [23, 24]. Limited reports were available on the densification of B_4C with pre-synthesized diboride powders (TiB_2, ZrB_2 and CrB_2) as ceramic additives [17, 25-27].

The present paper gives the results of investigations carried out on the effect of HfB_2 addition on the densification and properties of B_4C by hot-pressing method.

EXPERIMENTAL

Boron carbide (B_4C; 78.5 % B, 19.5 % C, < 1 % O, 0.02 % Fe, 0.02 % Si; 5.3 μm mean particle diameter; Boron Carbide India Pvt Ltd) and in-house synthesized [28] Hafnium diboride (HfB_2; purity: 99 %, 0.5 % O_2, 0.4 % C; 3.1 μm mean particle diameter) were used as the starting materials. 0 to 30 wt. % of HfB_2 was added to B_4C and the powder mixtures were allowed to mix homogenously in a motorized mortar and pestle

(Pulverisette 2, Fritsch, Germany) for 2 h. The homogenously mixed B_4C-HfB_2 composite powder was loaded into the 17 mm dia. graphite die and further the graphite die assembly was kept inside the hot-pressing chamber. The chamber was evacuated to 10^{-5} mbar vacuum level. Hot-pressing was carried out under dynamic vacuum condition at temperature of 2173 K for 1 h duration with 40 MPa mechanical pressure. After sintering, the samples were allowed to cool down to room temperature and measured for density by liquid displacement method. The dense compacts were polished to mirror finish using a series of diamond suspensions ranging from 15 - 0.5 μm grades (Struers, Denmark). X-ray diffraction (XRD; XRG 3000, Inel, France) was performed with Cu-Kα radiation to identify the crystalline phases. Selected samples were characterized for microstructures using scanning electron microscopy (SEM; MB 2300 CT/100, CAMSCAN, UK) with simultaneous elemental analysis by energy dispersive spectrometer (EDS; X-MAX 80, OXFORD, UK). Vickers hardness and fracture toughness were measured based on indentation technique with a load of 1.961 N and 9.807 N respectively and for dwell time of 15 s. Anstis methodology [29] was adopted for indentation fracture toughness calculation. Elastic modulus was determined using ultrasonic wave velocity technique (UT 340 pulser receiver system, UTEX Scientific Instrument Inc., Canada). Electrical resistivity of the developed composites was measured by the four probe method at temperatures between 298 K and 1373 K.

RESULTS AND DISCUSSION

Densification and microstructures

Table 1 shows the sinter density and mechanical property results of B_4C and B_4C-HfB_2 composites processed at 2173 K. Sinter density of monolithic B_4C was measured as 96 % ρ_{th}. On addition of 2.5 wt. % of HfB_2 to B_4C, the sinter density of the compact increases and reaches a value of 99 % ρ_{th}. Sinter densities of composites with higher content of HfB_2 remained same as 99 % (Figure 1). It has to be noted that around 3 % improvement in sinter density was realized on mere addition of 2.5 wt. % HfB_2 to B_4C and it remained substantially unaltered with respect to increased weight fraction of HfB_2 content. Zrozi et al. have reported that with the addition of 4 wt. % TiB_2 to B_4C, no increase in density was observed in B_4C-TiB_2 composite under similar processing conditions [30]. Wenbo et al. observed that the sinter density of B_4C increased on addition of ZrB_2 up to 30 vol. %, further increase of ZrB_2 addition resulted in slight reduction in the sinter density (97.8 %) of the compacts [26]. On the other hand, Baharvandi et al. reported about the increase in densification of B_4C on TiB_2 addition and mentioned TiB_2's role as a grain growth inhibitor [31]. Fully dense B_4C-HfB_2 composite was fabricated by in-situ processing of B_4C with HfO_2 as additive at 2173 K under 40 MPa mechanical pressure [21]; whereas in the present study, with HfB_2 addition, the highest density achieved was ~ 99 % ρ_{th}. Goldstein et al. has made similar observations while processing B_4C–ZrB_2 composite by an in-situ method [17].

X-ray diffraction pattern of sintered composites indicates the presence of B_4C and HfB_2 phases only (Figure 2), which emphasize the high temperature phase stability of HfB_2 with respect to B_4C. Figure 3 shows the scanning electron micrograph of 99 % dense B_4C–HfB_2 composite that indicates random distribution of bright phase particles in the dark matrix. Bright and dark phases were analysed to contain (a) hafnium (Hf) and

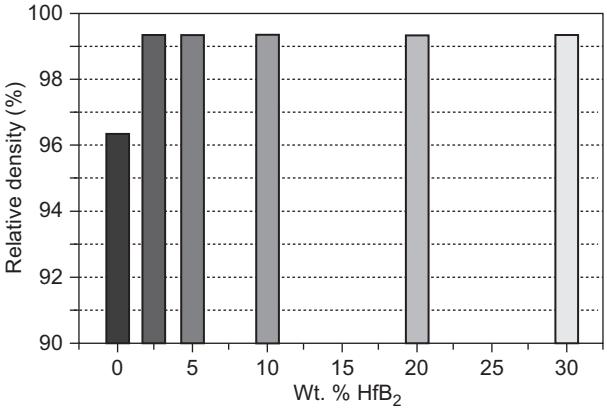

Figure 1. Relative densities of B_4C and B_4C–HfB_2 ceramics that was hot pressed at 2173 K under 40 MPa mechanical pressure.

Table 1. The sinter density and mechanical property results of B_4C and B_4C–HfB_2 hot pressed at 2173 K under 40 MPa mechanical pressure.

Sample composition	Theoretical density ($g \cdot cm^{-3}$)	Relative density (%)	Hardness (GPa)	Elastic modulus (GPa)	Fracture toughness ($MPa \cdot m^{1/2}$)
B_4C	2.52	96	36 ± 0.6	465 ± 7	2.3 ± 1.2
B_4C-2.5 wt. % HfB_2	2.56	99	35 ± 0.3	504 ± 5	3.6 ± 1
B_4C-5.0 wt. % HfB_2	2.60	99	32.6 ± 0.5	514 ± 15	4.4 ± 1.2
B_4C-10 wt. % HfB_2	2.69	99	30.9 ± 0.5	525 ± 20	5.5 ± 0.8
B_4C-20 wt. % HfB_2	2.89	99	29.5 ± 0.3	502 ± 10	6.6 ± 0.8
B_4C-30 wt. % HfB_2	3.12	99	28 ± 0.5	484 ± 5	7.1 ± 0.8

boron (B), and (b) boron (B) and carbon (C), respectively (Figure 4a-b). HfB_2 particles appear as a bright phase in the microstructure due to the larger atomic weight of Hf compared to B and C elements.

Certain advantages can be observed in sintering of B_4C with the addition of HfB_2 as compared to HfO_2. Though the in-situ processing route has proven to fabricate high dense B_4C composites, it often causes deviations from its stoichiometric composition [10, 19, 21]. This can be realized based on the reported changes in lattice parameters of B_4C phase in the sintered product with respect to oxide additions [10, 21]. Since both boron and carbon atoms taking part in the reduction of oxides, B/C ratio of B_4C will no longer remain the same as that of initial or starting material composition. In such cases, precise control over the material chemistry is often difficult. Further, the incomplete or partial completion of chemical reactions between B_4C and oxides would also cause compositional uncertainties in the material. B_4C finds many uses in nuclear industry as a neutron control rods, detectors etc. [1, 2]. The discrepancies that arise from compositional uncertainties, particularly impurities and non-stoichiometry are of primary concern for nuclear applications. Hence applications of this type, demand materials whose compositions and impurity levels are precisely known [1]. Table 2 shows the measured lattice parameters of B_4C phase that remain unaffected with respect to HfB_2 addition. Hence,

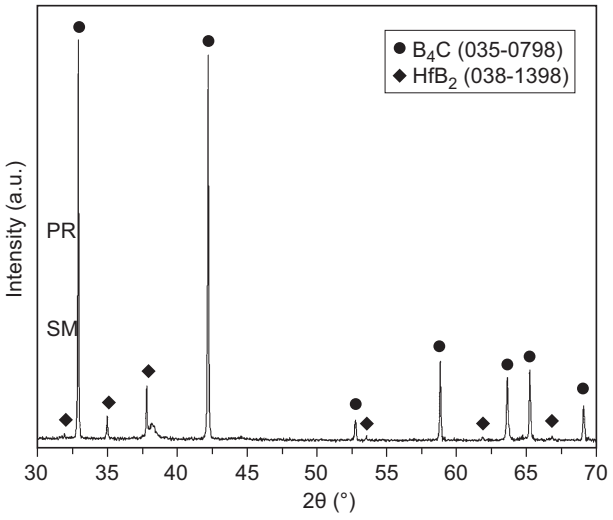

Figure 2. X-ray diffraction pattern of sintered B_4C-30 wt. % HfB_2 composite indicating the presence of B_4C and HfB_2 as the major phases.

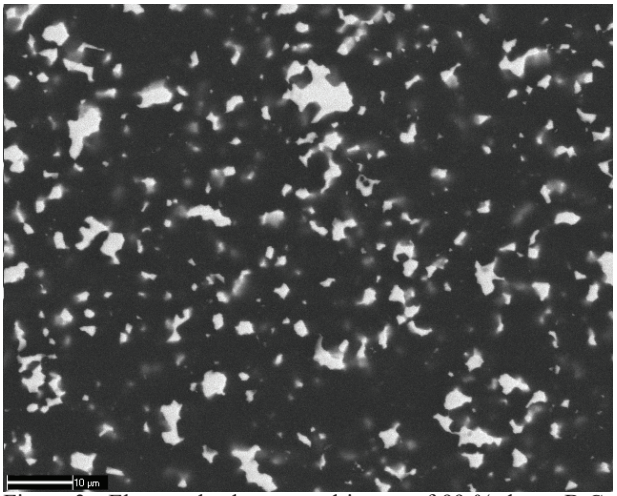

Figure 3. Electron back scattered image of 99 % dense B_4C-30 wt. % HfB_2 composite showing the random distribution of bright phase (HfB_2) in the dark matrix (B_4C).

Table 2. Lattice parameters of sintered B_4C compacts as a function of HfB_2 addition.

Sample Composition	Lattice parameters of B_4C phase	
	a (Å)	*c* (Å)
B_4C	5.6461	12.1116
B_4C-2.5 wt. % HfB_2		
B_4C-5.0 wt. % HfB_2		
B_4C-10 wt. % HfB_2		
B_4C-20 wt. % HfB_2		
B_4C-30 wt. % HfB_2		

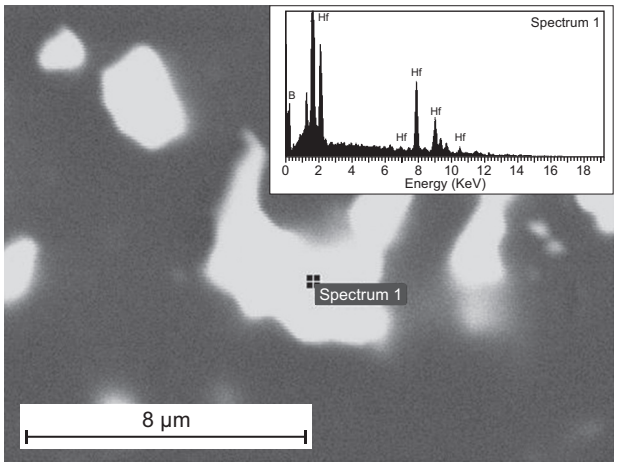

a)

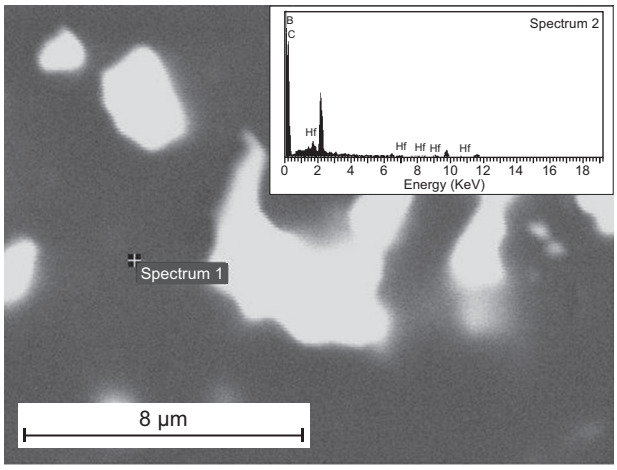

b)

Figure 4. EDS spot analysis spectrum indicating: a) Hafnium and Boron and b) Boron and Carbon as the constituting elements in the bright and dark regions respectively.

the direct additions HfB_2 could be preferred over the HfO_2 addition while fabricating boron carbide-hafnium diboride composites for nuclear applications.

Mechanical properties

Hardness of 96 % ρ_{th} B_4C was measured as 36 GPa. On addition of 2.5 wt. % HfB_2 to B_4C, the hardness of the composite material reduced to 35 GPa. Further increase of HfB_2 content to 30 wt. % has resulted in decreasing the hardness value to 28 GPa (Figure 5). The lower hardness of the developed B_4C-HfB_2 composite was mainly due to addition of reinforcement phase (HfB_2) which is relatively soft compared to monolithic B_4C. Elastic modulus of monolithic B_4C is measured as 465 GPa whereas the modulus of B_4C-HfB_2 composites were measured to be in the range of 485 - 525 GPa. Elastic modulus increases with increasing HfB_2 content up to 10 wt. % HfB_2 and reaches a maximum of 525 GPa (Figure 6). Further increase of HfB_2 up to 30 wt. % resulted in lowering the elastic modulus of B_4C-HfB_2 composite.

Indentation fracture toughness of monolithic B_4C and B_4C–HfB_2 composites were measured to be 2.3 MPa $m^{1/2}$ and 3 - 7 MPa·$m^{1/2}$ respectively (Figure 7). Fracture toughness increases with increasing addition of HfB_2 and reaches a maximum of ~7 MPa·$m^{1/2}$ (for 30 wt. % HfB_2) which is 3 times superior to that of monolithic B_4C. The observed increase in fracture toughness of the composite is mainly due to the crack tip deflections at the reinforced HfB_2 particles as shown in Figure 8a-c. In addition to crack deflection, the stress intensity factor at the crack tip reduces as it experiences compressive stresses [21, 32] while traversing through B_4C matrix and thus contributes for enhancing the fracture toughness of the material. The developed B_4C-30 wt. % HfB_2 composite exhibited a fracture toughness of 7.1 MPa·$m^{1/2}$ which is superior to some of the established boron carbide-boride composites such as B_4C-10 % HfB_2, B_4C-15 vol. % TiB_2, B_4C-TiB_2-Mo and B_4C-$MoSi_2$ whose fracture toughness values were reported to be 5.24, 6.1, 4.3 and 4.8 MPa·$m^{1/2}$ respectively [13, 33-35]. With improved fracture resist behaviour of B_4C-HfB_2 composite as well as the inherent neutron absorption characteristics of Hf, particularly in the epithermal region, this composite can be a potential substitute for monolithic B_4C as a neutron absorbers in nuclear reactors.

Electrical properties

The voltage and current characteristics of B_4C and B_4C-HfB_2 composite at temperatures 298 K, 773 K and 1273 K is shown in Figure 9. Figure 10 shows the electrical conductivity of B_4C and its dependence on HfB_2 content at different temperatures. At 298 K, the electrical conductivity of B_4C was measured to be 212 $\Omega^{-1}\cdot m^{-1}$.

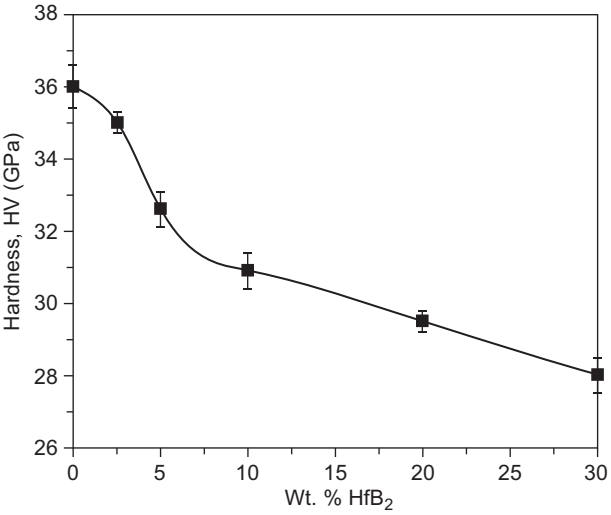

Figure 5. The effect of HfB_2 addition on hardness of B_4C.

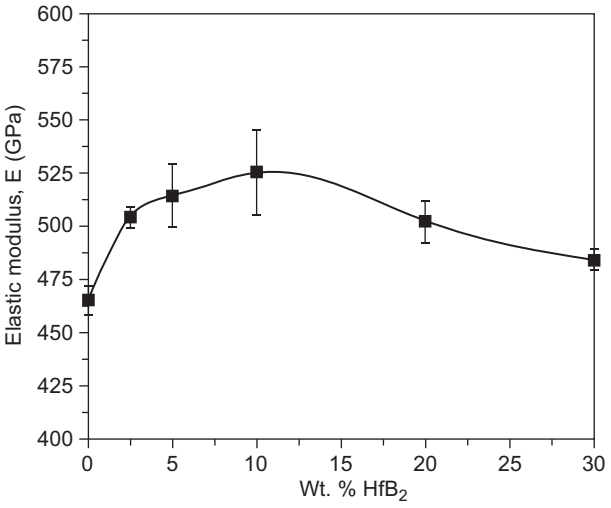

Figure 6. Variation of elastic modulus of B_4C with respect to HfB_2 addition.

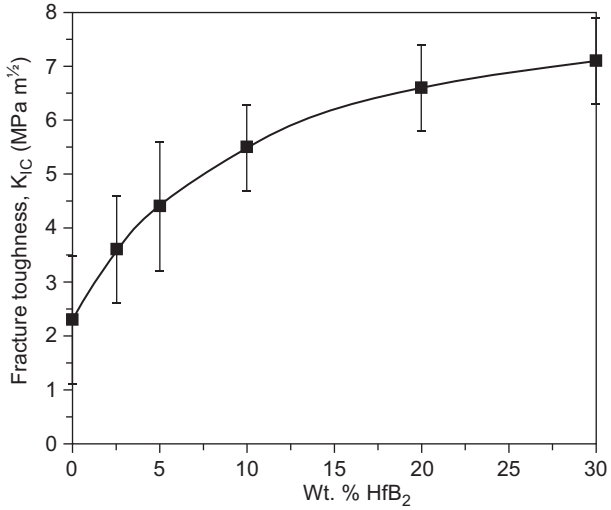

Figure 7. Effect of HfB_2 addition on fracture toughness of B_4C.

With increasing temperature, the electrical conductivity was found to increase and attained 2813 $\Omega^{-1}\cdot m^{-1}$ at 773 K which is one order increase in conductivity compared to that of room temperature value. On further increasing the temperature to 1373 K, the conductivity of B_4C was measured to be 5639 $\Omega^{-1}\cdot m^{-1}$ which is approximately twice the value of conductivity that was measured at 773 K. Overall, the monolithic B_4C has shown 25 times the initial conductivity value on increasing the temperature from 298 K to 1373 K. At 298 K, the electrical conductivity of B_4C sample containing 2.5 wt. % HfB_2 was measured as 340 $\Omega^{-1}\cdot m^{-1}$ which is 60 % higher than the conductivity of monolithic B_4C. It was observed the reinforcement of HfB_2 to B_4C matrix enhances

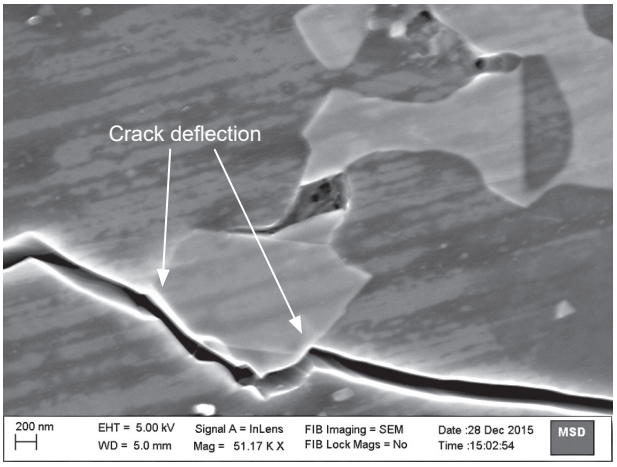

a)

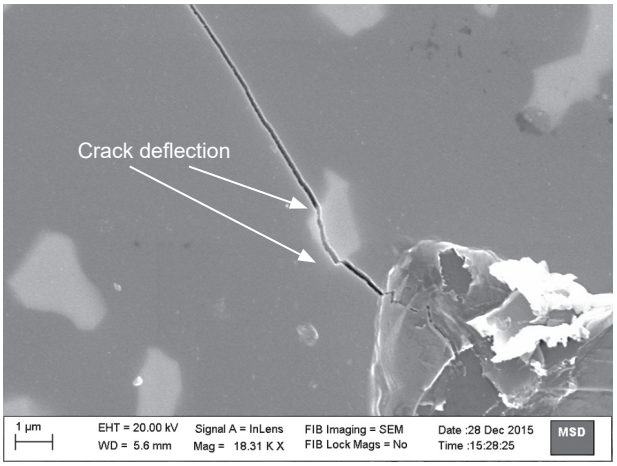

b)

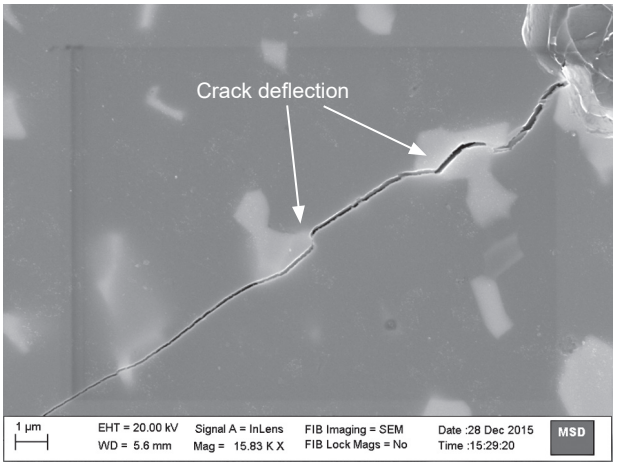

b)

Figure 8. Microstructures of 99 % dense B_4C-30 wt. % HfB_2 composite showing the deflection of crack propagation path due to the existence of second phase particle.

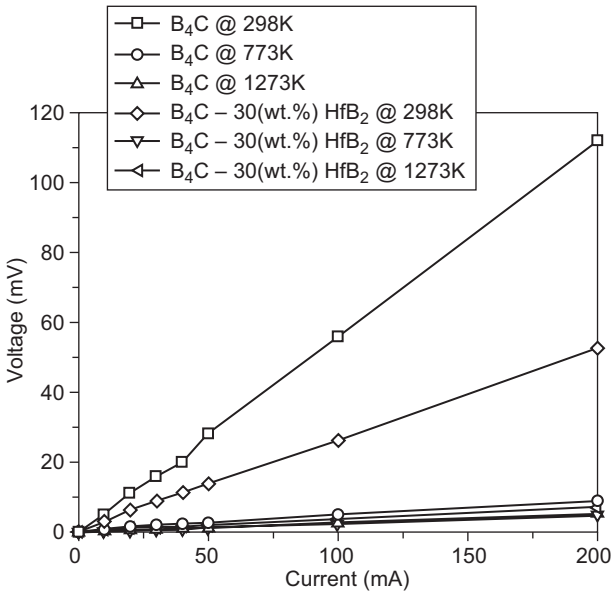

Figure 9. Voltage and current characteristics of B_4C and B_4C-30 wt. % HfB_2 composite at temperatures 298 K, 773 K and 1273 K.

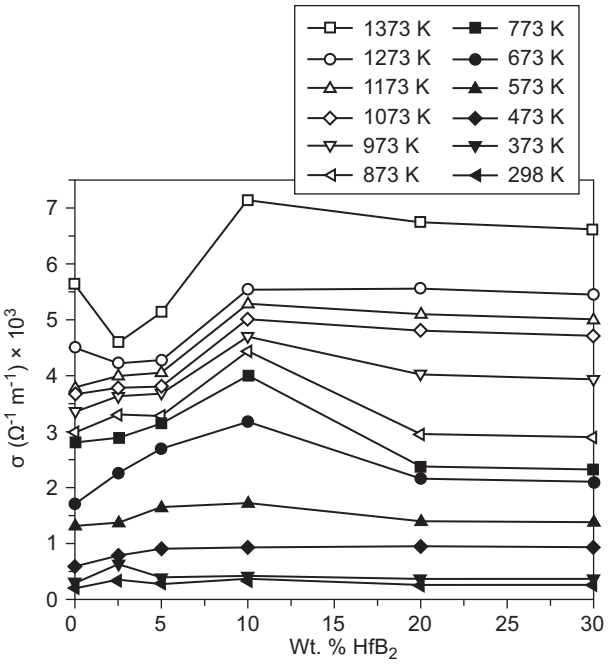

Figure 10. The electrical conductivity (σ) of B_4C and its dependence on HfB_2 content at different temperatures (298 K to 1373 K).

the room temperature electrical conductivity of the material. This is due to the fact that the HfB_2 is a better conductor at room temperature than B_4C and hence, the overall conductivity of the composite was increased. Electrical conductivities of B_4C containing different proportion of HfB_2 was estimated based on Maxwell's equation, which is in line with the present observations (Figure 11). Similar trend in conduction has been reported when CrB_2 was added to B_4C [36]. Like TiB_2 and ZrB_2 ceramics, HfB_2 is known to exhibit metallic like conduction behaviour whose conductivity decreases with increase of temperature due to the increased scattering of conducting electrons by lattice phonons [23, 37-38]. Hence, due to reinforcement of HfB_2 to B_4C, it was expected that the conductivity of B_4C would decrease at high temperatures; but on the contrary, it increased with temperature. At 473 K, conductivity of the B_4C sample was measured to increase from 797 $\Omega^{-1}\cdot m^{-1}$ to 936 $\Omega^{-1}\cdot m^{-1}$ on addition of 2.5 and 10 wt. % of HfB_2 respectively. On further increase of HfB_2 content from 10 to 30 wt. %, the conductivity of B_4C remain unchanged at 473 K (B_4C - 30 wt. % HfB_2: 938 $\Omega^{-1}\cdot m^{-1}$); whereas conductivity measured at temperatures between 573 K and 1373 K showed a decreasing trend on increasing the HfB_2 content beyond 10 wt. % (Figure 10). B_4C samples containing 2.5 and 5 wt. % HfB_2 resulted in systematic rise in conductivities up to 1173 K, beyond this temperature, a slight dip in conductivity was noticed compared with monolithic B_4C. For all the tested temperatures between 298 K and 1373 K, B_4C with 10 wt. % HfB_2 content exhibited a highest conductivity compared with that of all the other compositions. The conductivity of B_4C-10 wt. % HfB_2 composite was measured as 7144 $\Omega^{-1}\cdot m^{-1}$ which is 26 % higher than monolithic B_4C (5639 $\Omega^{-1}\cdot m^{-1}$) and 8 % higher than B_4C-30 wt. % HfB_2 composite (6608 $\Omega^{-1}\cdot m^{-1}$) at 1373 . Dolor et al. made similar observations during the investigation of high temperature electrical properties of B_4C-HfB_2 system and reported the maximum in con-ductivity with 10 wt. % HfB_2 at 1000 K [39]. Further he articulated this anomalous behaviour to the lower sinter density of sample that contained 10 wt. % HfB_2 compared with other compositions. In the present study, all the tested samples had identical sinter densities (~ 99 % ρ_{th}) but still exhibited the similar behaviour. Hence the remark over density effects on this anomalous behaviour in conductivity could be considered invalid. The electrical conductivity of the composites is dependent on several factors including the intrinsic conductivity of matrix and particulates, its volume fraction, size, shape, distributions and porosity. These parameters were not fully investigated in this study.

Figure 12 shows the plot of log σT versus 1/T that exhibit nearly a linear relationship for both B_4C and B_4C-HfB_2 composites. The activation energy of B_4C was calculated to be 0.163 eV which indicates the domination of bipolaron hopping during electrical conduction; whereas activation energies of B_4C containing 2.5 to 30 wt. % HfB_2 were ranged between 0.14 - 0.16 eV. In the present study, the activation energy reported for B_4C is consistent with the literature reported values (0.14 - 0.17 eV) [40-42]. These calculated activation energies for composites are more close to the value of monolithic B_4C which suggests that the electrical conduction in B_4C composites would primarily occur through B_4C grains with bipolaron hopping as the con-duction mechanism. The temperature coefficient of electrical resistance (TCER) values were calculated to be 1.03×10^{-3} K^{-1} for B_4C and 1.54×10^{-3} K^{-1} for B_4C-30 wt. % HfB_2. The TCER values of the composites ranged between 1.2 to 1.64 except for 10 wt. % HfB_2 composition. TCER of B_4C-HfB_2 composites is given in Table 3 which indicates a maximum value of 2.23×10^{-3} K^{-1} corresponding to 10 wt. % HfB_2 addition. The change in conductivity with respect to temperature

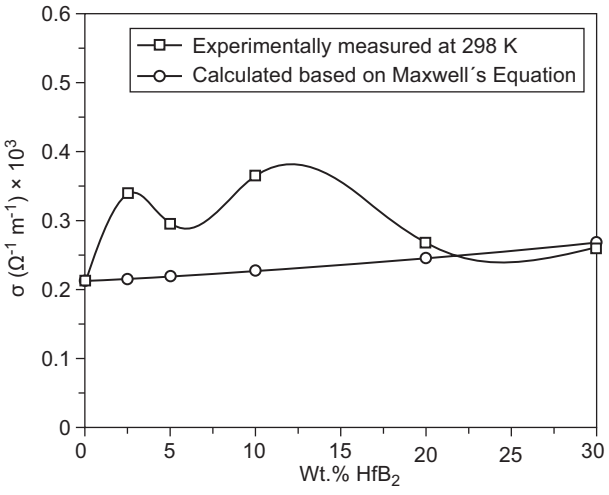

Figure 11. Comparison of experimentally measured and estimated room temperature electrical conductivity (σ) of B_4C specimens as a function of HfB_2 content.

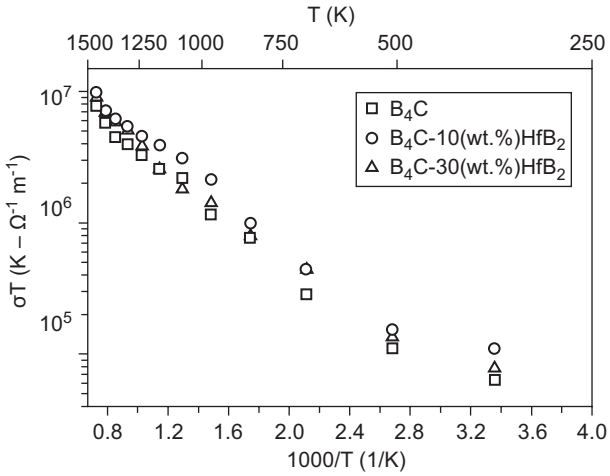

Figure 12. Plot of log (σT) versus reciprocal of temperature for B_4C with 0 wt. %, 10 wt.% and 30 wt.% HfB_2.

Table 3. Temperature coefficient of electrical resistance (TCER) of monolithic B_4C and B_4C–HfB_2 composites

Composition	TCER (10^{-3} K^{-1})
B_4C	1.03
B_4C-2.5 wt. % HfB_2	1.42
B_4C-5 wt. % HfB_2	1.29
B_4C-10 wt. % HfB_2	2.23
B_4C-20 wt. % HfB_2	1.61
B_4C-30 wt. % HfB_2	1.54

is found to be predominant for B_4C-10 wt. % HfB_2 composite compared to other proportions including monolithic B_4C.

CONCLUSION

- In the present study, 99 % dense B_4C-HfB_2 was fabricated by hot-pressing route with the following processing conditions: Temperature of 2173 K under 40 MPa mechanical pressure for 1 h dwell time.
- Hardness, elastic modulus and fracture toughness of B_4C-HfB_2 composites were measured to be in the range of 36 - 28 GPa, 465-525 GPa and 2.3 - 7.1 $MPa{\cdot}m^{1/2}$ respectively. With increasing HfB_2 content, hardness decreases and fracture toughness increases. B_4C-10 wt. % HfB_2 exhibited a maximum elastic modulus of 525 GPa.
- Crack deflection was observed and attributed to be the primary toughening mechanism for B_4C-HfB_2 composites.
- Electrical conductivity of both B_4C and B_4C-HfB_2 composites increases with increase in temperature. B_4C containing 10 wt. % HfB_2 exhibited a maximum conductivity of 7144 $\Omega^{-1}{\cdot}m^{-1}$ at 1373 K. Activation energy of B_4C-HfB_2 composites were measured to be in the range of 0.14 - 0.16 eV.

Acknowledgments

The author wishes to thank Shri. C. Subramanian, Ex-Scientist and Raja Ramanna Fellow, BARC for sharing the valuable inputs during hot pressing process. Author also thankful to Dr. R. C. Hubli, former Head MPD, BARC for his support during the project work.

REFERENCES

1. Thevenot F. (1990): Boron carbide – a comprehensive review. *Journal of the European Ceramic society*, *6*(4), 205-225. doi:10.1016/0955-2219(90)90048-K
2. Suri A.K., Subramanian C., Sonber J.K., Murthy T.C. (2010): Synthesis and consolidation of boron carbide: a review. *International Materials Reviews*, *55*(1), 4-40. doi :10.1179/095066009X12506721665211
3. Angers R., Beauvy M. (1984): Hot-pressing of boron carbide. *Ceramics international*, *10*(2), 49-55. doi:10.1016/0272-8842(84)90025-7
4. Kuzenkova M.A., Kislyi P.S., Grabchuk B.L., Bodnaruk N.I. (1979): The structure and properties of sintered boron carbide. *Journal of the Less Common Metals*, *67*(1), 217-223. doi:10.1016/0022-5088(79)90095-X
5. Dole S.L., Prochazka S., Doremus R.H. (1989): Microstructural coarsening during sintering of boron carbide. *Journal of the American Ceramic Society*, *72*(6), 958-966. doi:10.1111/j.1151-2916.1989.tb06252.x
6. Roy T.K., Subramanian C., Suri A.K. (2006): Pressureless sintering of boron carbide. *Ceramics International*, *32*(3), 227-233. doi:10.1016/j.ceramint.2005.02.008
7. Schwetz K.A., Grellner W. (1981): The influence of carbon on the microstructure and mechanical properties of sintered boron carbide. *Journal of the Less Common Metals*, *82*, 37-47. doi:10.1016/0022-5088(81)90195-8
8. Tkachenko Y.G., Britun V.F., Prilutskii E.V., Yurchenko D.Z., Bovkun G.A. (2005): Structure and properties of B_4C-SiC composites. *Powder Metallurgy and Metal Ceramics*, *44*(3-4), 196-201. doi:10.1007/s11106-005-0080-8
9. Champagne B., Angers R. (1979): Mechanical Properties of Hot-Pressed B-B_4C Materials. *Journal of the American Ceramic Society*, *62*(3-4), 149-153. doi:10.1111/j.1151-2916.1979.tb19042.x
10. Levin L., Frage N., Dariel M.P. (1999): The effect of Ti and TiO_2 additions on the pressureless sintering of B_4C. *Metallurgical and Materials Transactions A*, *30*(12), 3201-3210. doi:10.1007/s11661-999-0230-6
11. Goldstein A., Geffen Y., Goldenberg A. (2001): Boron carbide–zirconium boride in situ composites by the reactive pressureless sintering of boron carbide–zirconia mixtures. *Journal of the American Ceramic Society*, *84*(3), 642-644. doi:10.1111/j.1151-2916.2001.tb00714.x
12. Huang S.G., Vanmeensel K., Van der Biest O., Vleugels J. (2011): In situ synthesis and densification of submicrometer-grained B_4C–TiB_2 composites by pulsed electric current sintering. *Journal of the European Ceramic Society*, *31*(4), 637-644. doi:10.1016/j.jeurceramsoc.2010.10.028
13. Skorokhod V., Krstic V.D. (2000): High strength-high toughness B_4C-TiB_2 composites. *Journal of Materials Science Letters*, *19*(3), 237-239. doi:10.1023/A:1006766910536
14. Yue X., Zhao S., Lü P., Chang Q., Ru H. (2010): Synthesis and properties of hot pressed B_4C-TiB_2 ceramic composite. *Materials Science and Engineering: A*, *527*(27), 7215-7219. doi:10.1016/j.msea.2010.07.101
15. Grigor'ev O.N., Koval'chuk V.V., Zaporozhets O.I., Bega N.D., Galanov B.A., Prilutskii É.V., Kotenko V.A., Kutran' T.N., Dordienko N.A. (2006): Synthesis and physicomechanical properties of B_4C-VB_2 composites. *Powder Metallurgy and Metal Ceramics*, *45*(1-2), 47-58. doi:10.1007/s11106-006-0041-x
16. Subramanian C., Roy T.K., Murthy T.C., Sengupta P., Kale G.B., Krishnaiah M.V., Suri A.K. (2008): Effect of zirconia addition on pressureless sintering of boron carbide. *Ceramics International*, *34*(6), 1543-1549. doi:10.1016/j.ceramint.2007.04.017
17. Goldstein A., Yeshurun Y., Goldenberg A. (2007): B_4C/metal boride composites derived from B_4C/metal oxide mixtures. *Journal of the European Ceramic Society*, *27*(2), 695-700. doi:10.1016/j.jeurceramsoc.2006.04.042

18. Sairam K., Sonber J. K., Murthy T.C., Subramanian C., Fotedar R.K., Nanekar P., Hubli R.C. (2014): Influence of spark plasma sintering parameters on densification and mechanical properties of boron carbide. *International Journal of Refractory Metals and Hard Materials*, *42*, 185-192. doi:10.1016/j.ijrmhm.2013.09.004
19. Larsson P., Axen N., Hogmark S. (2000): Improvements of the microstructure and erosion resistance of boron carbide with additives. *Journal of materials science*, *35*(14), 3433-3440. doi:10.1023/A:1004888522607
20. Telle R., Petzow G. (1988): Strengthening and toughening of boride and carbide hard material composites. *Materials Science and Engineering: A*, *105*, 97-104. doi:10.1016/0025-5416(88)90485-5
21. Sairam K., Sonber J.K., Murthy T.C., Subramanian C., Hubli R. C., Suri A.K. (2012): Development of B_4C–HfB_2 composites by reaction hot pressing. *International Journal of Refractory Metals and Hard Materials*, *35*, 32-40. doi:10.1016/j.ijrmhm.2012.03.004
22. Sairam K., Murthy T.S.R.Ch., Sonber J.K., Subramanian C., Hubli R.C., Suri A.K. (2014). Mechanical properties of HfB_2 reinforced B_4C matrix ceramics processed by in situ reaction of B_4C, HfO_2 and CNT. In: Udomkichdecha W., Böllinghaus Th., Manonukul A., Lexow J. (eds.): *Materials Challenges and Testing for Manufacturing, Mobility, Biomedical Applications and Climate.* Springer International Publishing, pp.87-96. doi:10.1007/978-3-319-11340-1_9
23. Fahrenholtz W.G., Hilmas G.E., Talmy I.G., Zaykoski J.A. (2007). Refractory diborides of zirconium and hafnium. *Journal of the American Ceramic Society*, *90*(5), 1347-1364. doi:10.1111/j.1551-2916.2007.01583.x
24. Ordan'yan S.S., Dmitriev A.I. (1989): Interaction in the system B_4C-HfB_2. *Powder Metallurgy and Metal Ceramics*, *28*(5), 424-426. doi:10.1007/BF00795052
25. Yamada S., Hirao K., Sakaguchi S., Yamauchi Y., Kanzaki S. (2002): Microstructure and mechanical properties of B_4C-CrB_2 ceramics. *Key Engineering Materials*, *206*, 811-814. doi:10.4028/www.scientific.net/KEM.206-213.811
26. Wenbo H., Jiaxing G., Jihong Z., Jiliang Y. (2013): Microstructure and properties of B_4C–ZrB_2 ceramic composites. *International Journal of Engineering and Innovative Technology*, *3*(1), 163-166.
27. Sigl L.S., Kleebe H.J. (1995): Microcracking in B_4C-TiB_2 composites. *Journal of the American Ceramic Society*, *78*(9), 2374-2380. doi:10.1111/j.1151-2916.1995.tb08671.x
28. Sonber J.K., Murthy T.C., Subramanian C., Kumar S., Fotedar R.K., Suri A.K. (2010): Investigations on synthesis of HfB_2 and development of a new composite with $TiSi_2$. *International Journal of Refractory Metals and Hard Materials*, *28*(2), 201-210. doi:10.1016/j.ijrmhm.2009.09.005
29. Anstis G.R., Chantikul P., Lawn B.R., Marshall D.B. (1981): A critical evaluation of indentation techniques for measuring fracture toughness: I, direct crack measurements. *Journal of the American Ceramic Society*, *64*(9), 533-538. doi:10.1111/j.1151-2916.1981.tb10320.x
30. Zorzi J.E., Perottoni C.A., Da Jornada J.A.H. (2005): Hardness and wear resistance of B_4C ceramics prepared with several additives. *Materials Letters*, *59*(23), 2932-2935. doi:10.1016/j.matlet.2005.04.047
31. Baharvandi H.R., Hadian A.M., Alizadeh A. (2006): Processing and mechanical properties of boron carbide–titanium diboride ceramic matrix composites. *Applied Composite Materials*, *13*(3), 191-198. doi:10.1007/s10443-006-9012-0
32. Taya M., Hayashi S., Kobayashi A.S., Yoon H.S. (1990): Toughening of a Particulate-Reinforced Ceramic-Matrix Composite by Thermal Residual Stress. *Journal of the American Ceramic Society*, *73*(5), 1382-1391. doi:10.1111/j.1151-2916.1990.tb05209.x
33. Radev D.D. (2010): Pressureless sintering of boron carbide-based superhard materials. *Solid State Phenomena*, *159*, 145-148. doi:10.4028/www.scientific.net/SSP.159.145
34. Jianxin D., Junlong S. (2009): Microstructure and mechanical properties of hot-pressed B_4C/TiC/Mo ceramic composites. *Ceramics International*, *35*(2), 771-778. doi:10.1016/j.ceramint.2008.02.014
35. Kumar S., Sairam K., Sonber J.K., Murthy T.C., Reddy V., Rao G.N., Rao T.S. (2014): Hot-pressing of $MoSi_2$ reinforced B_4C composites. *Ceramics International*, *40*(10), 16099-16105. doi:10.1016/j.ceramint.2014.06.135
36. Yamada S., Hirao K., Yamauchi Y., Kanzaki S. (2003): Mechanical and electrical properties of B_4C-CrB_2 ceramics fabricated by liquid phase sintering. *Ceramics international*, *29*(3), 299-304. doi:10.1016/S0272-8842(02)00120-7
37. Zhang L., Pejaković D.A., Marschall J., Gasch M. (2011): Thermal and Electrical Transport Properties of Spark Plasma-Sintered HfB_2 and ZrB_2 Ceramics. *Journal of the American Ceramic Society*, *94*(8), 2562-2570. doi:10.1111/j.1551-2916.2011.04411.x
38. Li X., Manghnani M.H., Ming L.C., Grady D.E. (1996): Electrical resistivity of TiB_2 at elevated pressures and temperatures. *Journal of Applied Physics*, *80*(7), 3860-3862. doi:10.1063/1.363341
39. Dolor J.I. (2015): Investigation of the Thermoelectric Properties of Boron Carbide-Hafnium Diboride Composite Materials. In: *NNIN REU Research Accomplishments*. Cornell University. pp. 92-93. http://www.nnin.org/sites/default/files/2015_REU/2015NNINreuRA_PDFs/2015NNINreuRA_Innocent-Dolor.pdf
40. Wood C., Emin D. (1984): Conduction mechanism in boron carbide. *Physical Review B*, *29*(8), 4582. doi:10.1103/PhysRevB.29.4582
41. Aselage T.L., Tallant D.R., Gieske J.H., Van Deusen S.B., Tissot R.G. (1990). Preparation and properties of icosahedral borides. In Freer R. (ed.): *The Physics and Chemistry of Carbides, Nitrides and Borides*. Kluwer, Dordrecht, NATO ASI Series,184, pp. 97-111.
42. Emin, D. (1986). Electronic transport in boron carbides. *AIP Conference Proceedings*,*140*, 189-205. doi:10.1063/1.35593